STRUCTURES, PROPERTIES AND TOPOLOGIES OF TWO LAYERED COMPOUNDS BASED ON 2-CARBOXETHYL(PHENYL)PHOSPHINIC ACID

B. Liu[1], Z.-H. Zhang[2], L. Xu[1,2], H. Jiao[2]

[1]*College of Chemistry and Chemical Engineering, Shaanxi University of Sciences and Technology, Xi'an, Shaanxi, P. R. China*
 E-mail: bliu_1203@163.com
[2]*Key Laboratory of Macromolecular Science of Shaanxi Province, School of Chemistry & Chemical Engineering, Shaanxi Normal University, Xi'an, Shaanxi, P. R. China*
 E-mail: xuling@snnu.edu.cn

Hydrothermal syntheses of 2-carboxyethyl(phenyl)phosphinic acid (H_2CEPPA) with $Bi(NO_3)_3$ and $Cd(NO_3)_2$ produce two layered complexes $[Bi_2(\mu_3\text{-}O)(CEPPA)_2]_n$ (**1**) and $[Cd(HCEPPA)_2]_n$ (**2**). Compound **1** is comprised of $[Bi_4(\mu_3\text{-}O)_2(POO)_4(COO)_4]$ SBUs which grow into a double wave-like 2D layer with —CH_2CH_2— spacers. Compound **2** crystallizes in the orthorhombic noncentrosymmetric space group *Pca*2_1, exhibiting a double lattice-like layer. Through edge-to-face $d\cdots\pi$ stacking, a 3D supramolecular framework is formed based on 2D lattices. Topological analyses indicate that **1** and **2** have *sql* (or Shubnikov tetragonal plane net) and *kgd* (or Shubnikov (3.6.3.6) plane net) topological networks respectively. **1** and **2** are isolated as single crystal pure phases, which is confirmed by powder XRD. TGA shows high thermal stabilities with decomposition temperatures of **1** and **2** being 373 and 303 °C respectively. The fluorescent spectra exhibit fluorescence quenching in **1** and sharp emission at 292 nm in **2**, which is assigned to intraligand emission.

The recent decades have witnessed a flourish development in the research on coordination polymers or metal-organic frameworks (MOFs), due to not only the potential applications in functional materials, gas adsorption as well as catalysis, but their variety of intriguing structural architectures and topologies [1—6]. One of the strategies to realize the construction of anticipative coordination polymers is the selection of metal ions, and organic ligands [7—9]. However, it is still a great challenge to synthesize coordination polymers with predictable structures and properties [10, 11]. 2-Carboxyethyl(phenyl)phosphinic acid (H_2CEPPA) was selected as our ligand not only for its use as reactive flame retardant [12], but for the structural features that it has owing to two formally analogous phosphinate and carboxylate moieties at both ends of a flexible alkyl —CH_2CH_2— spacer, and a phenyl group bonded to the phosphinate moiety [13, 14]. Though there are only four O donor sites, the (H)CEPPA ligand with a flexible conformation can exhibit structural diversity even with the same dentate number [15—19]. As compared to single carboxylate or phosphinate moiety, the phosphinate moiety bonded to an organic group can be readily designed as an asymmetric building block for second-order of NLO materials. The bonding of the phosphinate moiety with a phenyl ring can be re-

garded as a dipolar or push-pull chromophore, which can also be a source of the second-order NLO effect [18]. The existence of phenyl provides a high thermal and oxidation stability, and a negligible effect on the mechanical properties of the material.

Our interest is the investigation of fabricating MOFs with desired properties. H$_2$CEPPA serves as a fully or partly deprotonated anionic ligand in the presented work. Herein, we report the syntheses and structures of two 2D layered compounds $[Bi_2(\mu_3\text{-}O)(CEPPA)_2]_n$ (**1**) and $[Cd(HCEPPA)_2]_n$ (**2**) whose sample purity, thermogravimetric and fluorescent properties were characterized, and the topological types were assigned.

EXPERIMENTAL

Materials and physical measurements. The reagents and solvents were used directly as supplied commercially without further purification. 2-carboxyethyl(phenyl)phosphinic acid was synthesized according to the literature procedure [20]. FT-IR spectra were collected from KBr pellets (Aldrich, >99 %, FT-IR grade) on a Bruker Tensor 27 FT-IR spectrometer in the range 4000—400 cm^{-1}. Thermogravimetric (TG) analyses were carried out in the N$_2$ atmosphere from 30 to 800 °C on a SDT Q600 V8.3 Build 101 instrument with a heating rate of 20 °C·min^{-1} and an N$_2$ flow rate of 40 cm^3·min^{-1}. Powder XRD data for the materials were collected at ambient temperature on a Rigaku D/Max-3c diffractometer (Japan) (Cu$K_{\alpha_{1,2}}$ radiation, $\lambda_1 = 1.540598$ Å and $\lambda_2 = 1.544426$ Å), equipped with an X′Celerator detector and a flat-plate sample holder in a Bragg—Brentano para-focusing optics configuration (40 kV, 50 mA). Intensity data were collected in the range $5 \leq 2\theta \leq 50°$ by the step counting method (step being 0.02°) in continuous mode.

Synthesis of $[Bi_2(\mu_3\text{-}O)(CEPPA)_2]_n$ (1). 0.2 mmol, 0.0257 g 3-amino-1H-1,2,4-triazole-5-carboxylic acid, 0.2 mmol, 0.0978 g Bi(NO$_3$)$_3$·6H$_2$O, and 0.2 mmol, 0.0429 g H$_2$CEPPA mixed with 15 ml H$_2$O were placed in a crystallization vial placed in a 25 ml Teflon-lined stainless-steel autoclave. The mixture was kept inside the furnace at 120 °C for 5 days, and then naturally cooled to ambient temperature. The colorless platelet crystals of **1** suitable for X-ray diffraction were collected after soak clearing with water and ethanol. Yield based on H$_2$CEPPA: 20.1 mg, 11.7 %. IR data (in KBr, cm^{-1}) for **1**: 3434(m), 3057(w), 2922(w), 1642(w), 1527(s), 1412(s), 1380(s), 1310(s), 1271(w), 1207(w), 1105(s), 1066(w), 1009(s), 939(w), 823(w), 791(w), 753(s), 695(m).

Synthesis of $[Cd(HCEPPA)_2]_n$ (2). The similar process as that of **1** using 0.2 mmol, 0.0140 g 1H-1,2,4-triazole, 0.2 mmol, 0.0428 g H$_2$CEPPA, 0.2 mmol, 0.0618 g Cd(NO$_3$)$_2$·4H$_2$O in 20 ml H$_2$O produced colorless prism crystals. Yield based on H$_2$CEPPA: 9.2 mg, 8.5 %. IR data (in KBr, cm^{-1}) for **2**: 3440(m), 3069(w), 2916(w), 2846(w), 1873(m), 1662(s), 1463(w), 1437(m), 1348(m), 1310(w), 1277(s), 1150(s), 1021(s), 798(m), 753(m), 689(m).

Single crystal X-ray diffraction. Single crystals of compounds **1**—**2** were manually harvested from crystallization vials and mounted on Hampton Research CryoLoops using FOMBLIN Y perfluoropolyether vacuum oil (LVAC 25/6, purchased from Aldrich) [21] with the help of a Stemi 2000 stereomicroscope equipped with Carl Zeiss lenses. Data were collected on a Bruker X8 Kappa APEX II charge-coupled device (CCD) area-detector diffractometer (MoK_α graphite-monochromated radiation, $\alpha = 0.71073$ Å) controlled by the APEX2 software package [22] and equipped with an Oxford Cryosystems Series 700 cryostream monitored remotely using Cryopad [23]. Images were processed using SAINT+ [24], and data were corrected for absorption by the multiscan semi-empirical method implemented in SADABS [25].

The structures of compounds **1**—**2** were solved by direct methods using the SHELXTL^{TM} package of crystallographic software [26] and refined by the full-matrix least-squares technique on F^2. All non-hydrogen atoms were refined anisotropically. Hydrogen atoms were located at geometrically calculated positions to their carrier atoms and refined with isotropic thermal parameters included in the final stage of the refinement. A summary of the structural determination and refinement for compounds **1** and **2** is listed in Table 1. The selected bond distances and bond angles of compounds **1** and **2** are listed in Table 2.

Crystallographic and structure refinement data for **1** *and* **2**

Empirical formula	$C_{18}H_{18}Bi_2O_9P$	$C_{18}H_{20}CdO_8P_2$
Color and habit	Colorless platelet	Colorless prism
Crystal size, mm	0.15×0.10×0.04	0.12×0.10×0.09
Crystal system	Monoclinic	Orthorhombic
Space group	$P2_1/c$	$Pca2_1$
a, b, c, Å	13.1692(6), 16.8068(7), 10.0608(4)	15.5536(5), 5.5291(2), 23.0532(9)
β, deg.	107.071(5)	90
V, Å^3	2128.67(16)	1982.52(12)
Z	4	4
Fw	858.22	538.68
D_{calcd}, g/cm^3	2.678	1.805
μ, mm^{-1}	16.711	1.307
$F(000)$	1576	1080
θ, deg.	3.46 to 25.03	3.54 to 25.03
Reflections measured / independent	8297 / 3719 ($R_{int} = 0.0730$)	5126 / 2374 ($R_{int} = 0.0231$)
Observed reflection [$I > 2\sigma(I)$]	2884	2238
Final R_1, wR_2 indices (obs.)	0.0489, 0.1075	0.0239, 0.0557
R_1, wR_2 indices (all)	0.0684, 0.1177	0.0271, 0.0582
S	1.010	1.059
$\Delta\sigma$ (max / min)	0.002 / 0.000	0.000 / 0.000
$\Delta\rho$(max / min), e/Å^3	2.482 / –2.570	0.325 / –0.456

$R_1 = (\sum||F_0| - |F_c|| / \sum|F_0|)$. $wR_2 = [\sum(w(F_0^2 - F_c^2)^2)/\sum(w|F_0^2|^2)]^{1/2}$.

CCDC-1025033 (**1**) and 1025034 (**2**) contain the supplementary crystallographic data of compounds **1** and **2**. These data can be obtained free of charge from the Cambridge Crystallographic Data Centre via www.ccdc.cam.ac.uk/ data_request/cif.

Topology. According to A.F. Wells′ topology definition [27] and the MOF structural features, the constructed SBUs and the —CH$_2$CH$_2$— spacers from the (H)CEPPA ligand are simplified as the nodes and the topology networks of compounds **1** and **2** were calculated using the ADS program of the TOPOS 4.0 Professional structure-topological program package [28].

RESULTS AND DISCUSSION

Structural description of [Bi$_2$(μ$_3$-O)(CEPPA)$_2$]$_n$ (1). The single crystal analysis reveals that **1** is a 2D coordination polymer, in which its asymmetric unit is comprised of two independent Bi(III) atoms, two fully deprotoned CEPPA^{2-} ligands, and one μ$_3$-O^{2-} anion. Five-coordinate Bi1 atom is bonded to four oxygen atoms as the base plane and the apical site is occupied by O1A to a distorted BiO$_5$ square pyramid. The maximum deviation of Bi1 is 0.1619 Å from the best least-square base plane built by O1, O2B, O4, and O9 atoms. The distorted BiO$_5$ square pyramid displays τ = 0.165 (τ = = (β – α)/60, where α and β are the two largest bond angles around the Bi1 center; τ = 0 for the ideal square pyramid) [29]. The Bi2 center is in a six-coordinated pentagonal pyramid, in which O3B, O5A, O6C, O7C, O8A shape its pentagonal base plane and O1 occupies the apical site (Fig. 1). The bond valence sums (BVS) of Bi1 and Bi2 given by the valence sum calculations are 3.055 and 3.044, showing that both Bi atoms are Bi(III) cations. Similar BVS calculation for O1 of 2.391 suggests that

T a b l e 2

Selected bond distances (Å) *and bond angles* (deg.) *of compounds* **1** *and* **2**

1

Bi1—O1A	2.105(2)	O1A—Bi1—O4	87.07(10)	O8A—Bi2—O5A	86.98(10)
Bi1—O4	2.284(3)	O1A—Bi1—O9	87.87(9)	O1—Bi2—O6C	89.72(10)
Bi1—O9	2.310(3)	O4—Bi1—O9	84.81(11)	O8A—Bi2—O6C	157.43(10)
Bi1—O2B	2.355(3)	O1A—Bi1—O2B	87.05(10)	O5A—Bi2—O6C	70.55(10)
Bi1—O1	2.375(3)	O4—Bi1—O2B	81.43(12)	O1—Bi2—O3B	84.32(10)
Bi1—Bi1A	3.6088(4)	O9—Bi1—O2B	165.55(11)	O8A—Bi2—O3B	79.35(11)
Bi2—O1	2.102(2)	O1A—Bi1—O1	72.83(11)	O5A—Bi2—O3B	164.97(9)
Bi2—O8A	2.249(3)	O4—Bi1—O1	155.65(9)	O6C—Bi2—O3B	122.70(11)
Bi2—O5A	2.271(3)	O9—Bi1—O1	107.49(10)	O1—Bi2—O7C	72.29(10)
Bi2—O6C	2.508(3)	O2B—Bi1—O1	83.87(11)	O8A—Bi2—O7C	147.93(10)
Bi2—O3B	2.601(4)	O1A—Bi1—Bi1A	38.96(8)	O5A—Bi2—O7C	116.60(9)
Bi2—O7C	2.621(3)	O4—Bi1—Bi1A	124.73(7)	O6C—Bi2—O7C	50.17(10)
		O9—Bi1—Bi1A	100.14(7)	O3B—Bi2—O7C	74.05(10)
		O2B—Bi1—Bi1A	84.24(8)	Bi2—O1—Bi1A	137.10(15)
		O1—Bi1—Bi1A	33.87(5)	Bi2—O1—Bi1	112.00(11)
		O1—Bi2—O8A	87.71(10)	Bi1A—O1—Bi1	107.17(11)
		O1—Bi2—O5A	88.95(10)		

2

Cd1—O5	2.172(3)	O5—Cd1—O1	177.31(14)	O6A—Cd1—O4C	93.50(11)
Cd1—O1	2.170(4)	O5—Cd1—O6A	88.45(12)	O2B—Cd1—O4C	82.07(12)
Cd1—O6A	2.304(3)	O1—Cd1—O6A	90.26(13)	O5—Cd1—O8D	94.16(13)
Cd1—O2B	2.335(3)	O5—Cd1—O2B	93.98(12)	O1—Cd1—O8D	88.04(14)
Cd1—O4C	2.353(4)	O1—Cd1—O2B	87.13(13)	O6A—Cd1—O8D	84.05(12)
Cd1—O8D	2.381(3)	O6A—Cd1—O2B	174.95(12)	O2B—Cd1—O8D	100.17(11)
		O5—Cd1—O4C	90.35(14)	O4C—Cd1—O8D	174.80(13)
		O1—Cd1—O4C	87.38(14)		

Symmetry codes: 1) A = –x+1, –y, –z+1; B = x, –y+1/2, z–1/2; C = x, –y–1/2, z–1/2. 2) A = x, y–1, z; B = x, y+1, z; C = x+1/2, –y, z; D = x–1/2, –y+1, z.

O1 is the O^{2-} anion. μ_3-O1 and O1A link two symmetric [Bi$_3$] units into a [Bi$_4$O$_2$] parallelogram with Bi1···Bi2 separations of 3.715 and 3.916 Å, and the diagonal Bi1···Bi1 separation is 3.609 Å. The [Bi$_4$O$_2$] parallelogram is further stabilized by two pairs of bidentate —POO$^-$ bridges bonding on the longer Bi1—Bi2 sides, one pair of bidentate —COO$^-$ groups on the shorter Bi1—Bi2 sides, and one pair of —COO$^-$ groups chelating on Bi2 centers, thus forming [Bi$_4$(μ_3-O)$_2$(POO)$_4$(COO)$_4$] SBU. These four [Bi$_4$(μ_3-O)$_2$(POO)$_4$(COO)$_4$] SBUs are further bridged by the other four —CH$_2$CH$_2$— spacers from CEPPA^{2-} ligands in the bis-bidentate bridging mode or bidentate/chelating bridging mode (Scheme 1) into a 28-membered ring, whose propagations produce both wave-like 2D layers along the *bc* plane and a further cross link at each [Bi$_4$(μ_3-O)$_2$(POO)$_4$(COO)$_4$] SBU into a double layer along the *bc* plane (Fig. 2). With the topology analysis of this framework, we will have a better insight into the structure. [Bi$_4$(μ_3-O)$_2$(POO)$_4$(COO)$_4$] SBU could be regarded as an 8-connected node, and another —CH$_2$CH$_2$— spacer from the CEPPA^{2-} ligand as a 2-connected bridge. The whole framework can be simplified as a double (4,4) topological net with the topological type being sql or Shubnikov tetragonal plane net (Fig. 2).
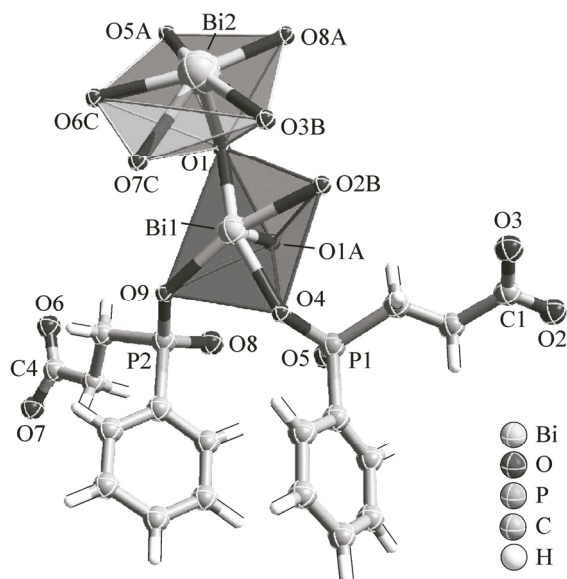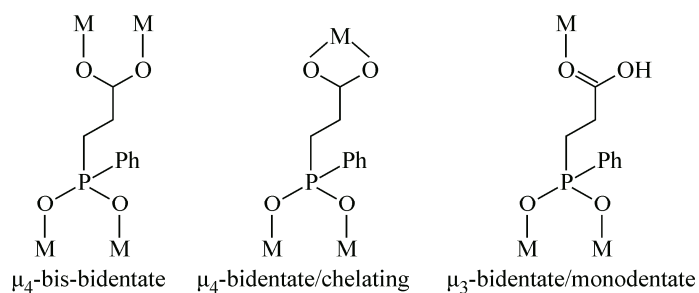
Fig. 1. Coordination spheres of Bi(III) centers with atom labeling in **1**.
Symmetry codes: A = –x+1, –y, –z+1;   B = x, –y+1/2, z–1/2;   C = x, –y–1/2, z–1/2

μ₄-bis-bidentate   μ₄-bidentate/chelating   μ₃-bidentate/monodentate

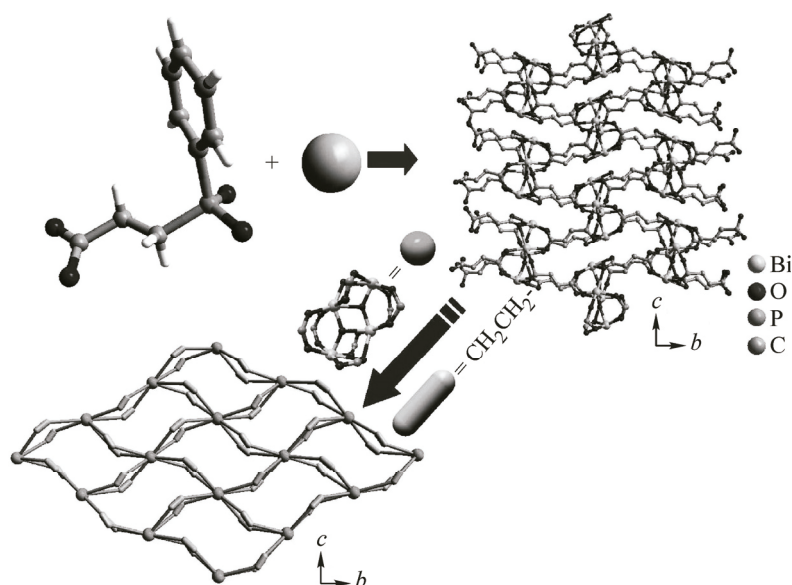Scheme 1. Coordination modes of (H)CEPPA ligands in compounds **1** and **2**

Fig. 2. 2D layer and *sql* topological network in compound **1**

Structural description of [Cd(HCEPPA)₂]ₙ (2). The structural analysis indicates that compound **2** features a 2D layer. Compound **2** crystallizes in the orthorhombic noncentrosymmetric space group *Pca*2₁ whose structural flack factor is –0.03(3) with 573 Friedel pairs, indicating that the absolute

Fig. 3. Coordination sphere of the Cd(II) center with atom labeling in compound **2**. Symmetry codes: A = *x*, *y*–1, *z*; B = *x*, *y*+1, *z*; C = *x*+1/2, –*y*, *z*; D = *x*–1/2, –*y*+1, *z*
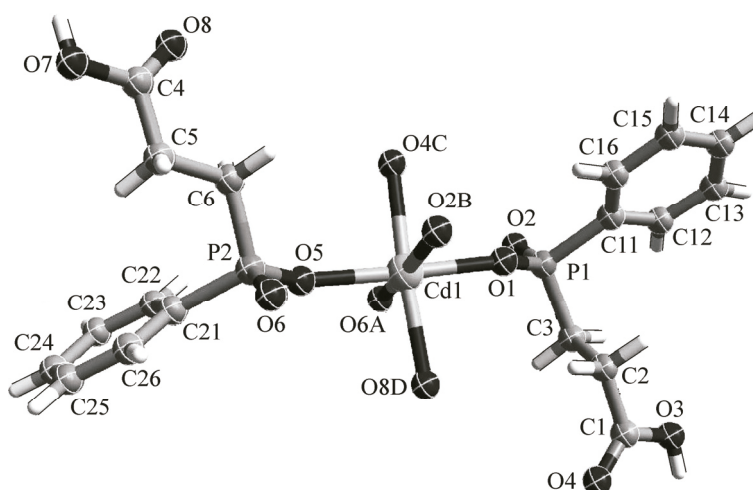
structure is accurate [30]. In the asymmetric unit of compound **2** there are one Cd(II) cation and two distinct HCEPPA$^-$ anions. The six-coordinated Cd(II) center locates in a slightly distorted octahedron, O2B, O4C, O6A, O8D form the equatorial plane with short Cd—O distances ranging within 2.304(3)—2.381(3) Å, and O1 and O5 occupy the axial vertices with the Cd—O distances of around 2.17 Å (Fig. 3). Due to the consideration of the charge balance and the coordination sphere of the Cd(II) center, —POOH groups of the H$_2$CEPPA ligand are deprotonated, however, —COOH groups are not deprotonated; that is, H$_2$CEPPA is partly deprotoned to HCEPPA$^-$. Two —POO$^-$ moieties connect two Cd(II) centers into a near-planar 8-membered ring through the bidentate bridging mode, and their growth along the *b* direction produces a lattice-like double chain. Interestingly, the same-type —POO$^-$ moieties slide along the *b* direction of the 1D chain, which is different from centro/axial/plane-symmetrical ones. Through the connections of the other monodentate alkyl carboxylate groups along the *a* direction, a double lattice-like layered network is shaped along the *ab* plane (Fig. 4). In the 2D layer there exist strong C—H···O hydrogen bondings (O3—H3C···O2 = 2.505(6), 178.3°; O7—H7A···O6 = 2.572(5), 178.1°; C5—H5B···O4 = 3.194(7) Å, 126.8°). A 3D supramolecular architect-
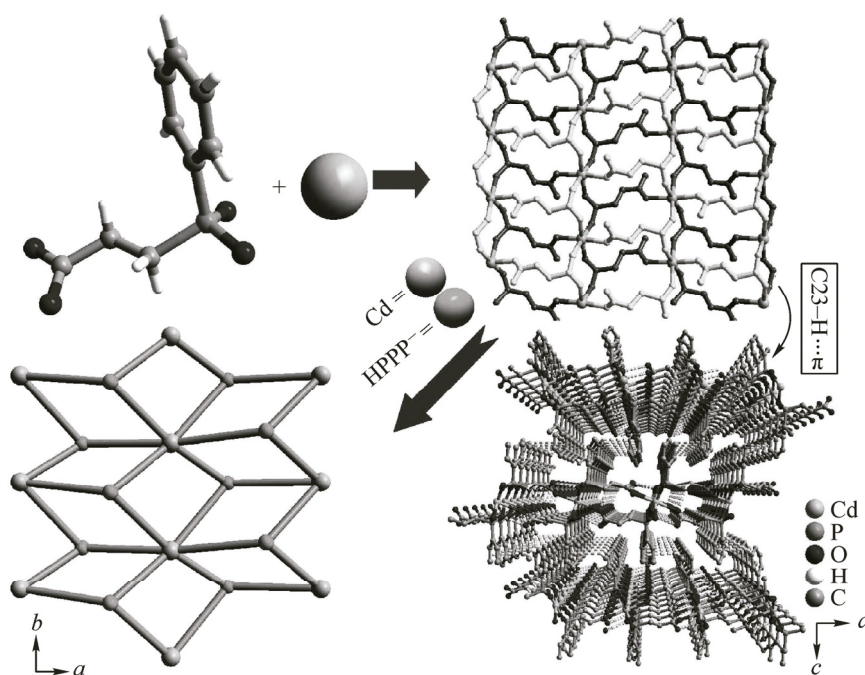

Fig. 4. 2D layer, *kgd* topological net, and 3D supramolecular framework in compound **2**

ture is formed and further stabilized through edge-to-face stacking interactions C23—H23A···π (3.470 Å, 122.99°, π = the centroid of phenyl containing C11). With the Cd(II) atom and the HCEPPA⁻ ligand being regarded as 6- and 3-connected nodes respectively, the whole 2D double network can be simplified as a common 2-nodal (3,6)-connected *kgd* topological net or Shubnikov plane (3.6.3.6) net (Fig. 4).

Compounds **1** and **2** were obtained from the similar synthetical processes with fixed ratios of re-actants, solvent, anion of metal salts, reaction time, and temperature. Some commons can be found between **1** and **2**. For example, **1** and **2** are both double layers; they tend to form dimeric rings in which two metal centers alternatively link two (H)CEPPA ligands. However, the selection of the metal center can be inferred as an essential factor to fabricate the final structures of the two coordination polymers. Because of the high Lewis acidity and expandable coordination sphere of Bi(III) [31, 32], it usually hydrolyzes into bulk bismuth-oxo clusters with —OH⁻ or O²⁻ as auxiliary ligands [33—37]. Meantime, the inherent difficulties in hydrolytic pathways, which hinder the control of compositions in the hydrothermal process, often result in different species forming mixtures [38, 39]. The hydro-lysis of the metal center also affects the degree of deprotonation of the ligand, thus forming different coordination modes. For instance, H_2CEPPA in **1** is fully deprotonated and exhibits two types of coor-dination modes (the bis-bidentate bridging mode and the bidentate/chelating bridging mode) while H_2CEPPA in **2** is partially deprotonated and has only one bidentate/monodentate coordination mode (Scheme 1). Therefore, the final 2D layered structures of compounds **1** and **2** are significantly different as a result of differences in the metal and coordination modes of (H)CEPPA ligands.

Powder XRD. The experimental powder XRD patterns for compounds **1** and **2** match well with those simulated from the single crystal structure data (Figs. 5 and 6), indicating that compounds **1** and **2** were isolated as single crystal pure phases.

FT-IR spectra. The asymmetric stretching vibrations $\upsilon_{as}(COO^-)$ were observed in the range 1527—1642 cm⁻¹ and symmetric stretching vibrations $\upsilon_s(COO^-)$ were observed in the range 1380—1412 cm⁻¹ for **1**; $\upsilon_{as}(COO^-)$ within 1463—1662 cm⁻¹ and $\upsilon_s(COO^-)$ within 1348—1437 cm⁻¹ for **2**. The above stretching vibrations were shifted to lower wavenumbers as compared to carbonyl frequen-cies of the free H_2CEPPA ligand ($\upsilon_{C=O}$ = 1730 cm⁻¹). The differences $\Delta(\upsilon_{as}(COO^-) - \upsilon_s(COO^-))$ were beyond 200 cm⁻¹, showing the existence of coordinated carboxylate groups [40—42], in accordance with the single crystal structural analysis. The peaks at 1105 cm⁻¹ for **1** and 1150 cm⁻¹ for **2** are from
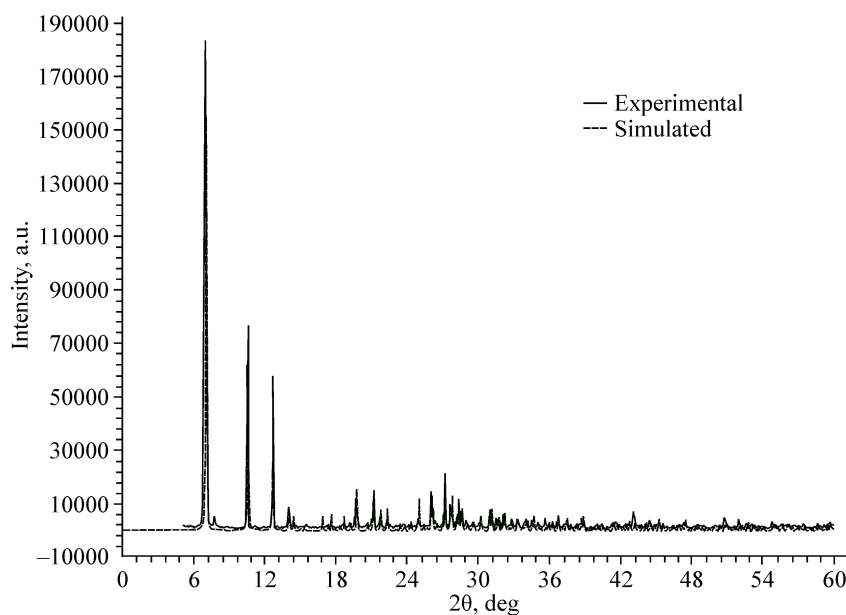

Fig. 5. Comparison of the powder XRD pattern of compound **1** with that simulated from single crystal structure data
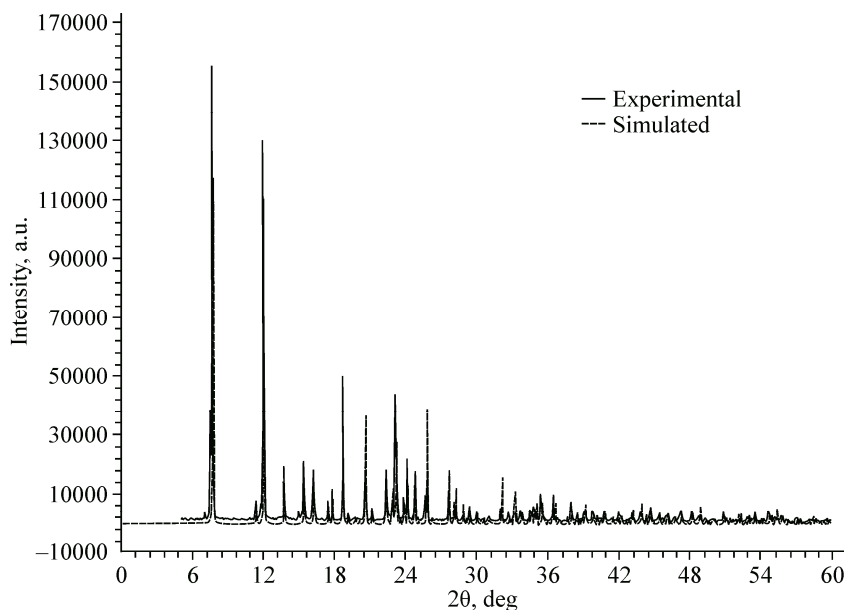
Fig. 6. Comparison of the powder XRD pattern of compound **2** with that simulated
from single crystal structure data

P=O stretching vibrations; blue-shifts appear after the coordination, as compared to $\upsilon_{P=O} = 1227$ cm^{-1} of the free H$_2$CEPPA ligand. The peaks at around 3440 cm^{-1} are assigned to $\upsilon_{C—H \cdots O}$.

TG analysis. TGA of compounds **1** and **2** show their thermal stabilities up to 300 °C; then the TGA curves exhibit two main steps of weight losses (Fig. 7). The first sharp weight losses start at decomposition temperatures of 373 and 303 °C for **1** and **2** respectively whereupon the decomposition of the (H)CEPPA ligand occurs followed by overlapped weight losses in the range of 417—597 and 365—550 °C for **1** and **2** respectively. The initial decomposition temperatures of both compounds are much higher than 187.5 °C of H$_2$CEPPA. The total weight losses of 33.2 and 57.5 % are close to the calculated values (35.4 % for **1** and 56.9 % for **2**) if the final residual products are assumed to be BiPO$_4$ and Cd(H$_2$PO$_4$)$_2$ respectively. The observation that the initial decomposition temperature of **1** is 70 °C higher than that of **2** indicates that **1** is much more stable than **2**, which should relate with the fact that there are more Bi—O bonds in **1** than Cd—O bonds in **2**, although the Cd—O bond energy is somewhat larger than that of Bi—O.

Fluorescence. The emission spectra of compounds **1** and **2** in the solid state were recorded at room temperature. The free H$_2$CEPPA ligand shows a single emission peak at 293 nm with excitation
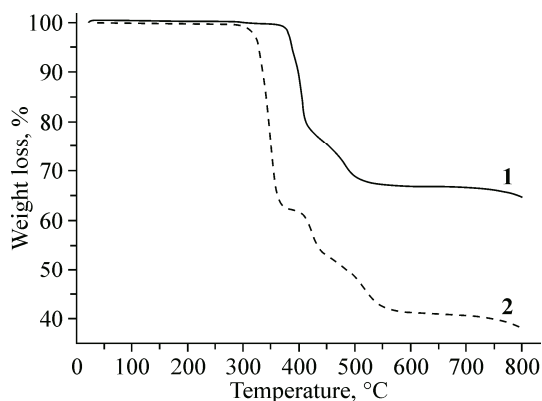

Fig. 7. TG curves of compounds **1** and **2**

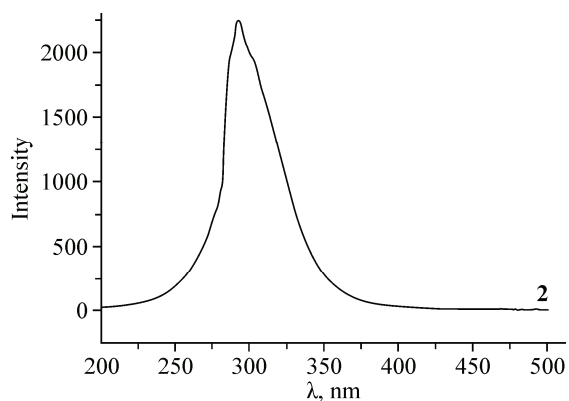*Fig. 8.* Solid-emission spectrum of **2** ($\alpha_{ex} = 271$ nm) recorded at room temperature

at 225 nm. However, fluorescence quenching occurs in compound **1**, suggesting that photons are absorbed by H_2CEPPA and the energy is transferred to Bi(III). However, Bi(III) is not always a fluorescence quenching agent, which is widely used in inorganic phosphors and coordination complexes [43—45]. Therefore, the reason for the fluorescence quenching may be the structural factor of the $[Bi_4O_2]^{8-}$ unit that accepts energy from H_2CEPPA, which is emitted as heat rather than the photon. The fluorescence quenching indicates that the coordination of H_2CEPPA to Bi(III) can prevent the ligand from being destroyed by ultraviolet light, and also stabilize the structure, which can be supported by the fact that the decomposition temperature of **1** is much higher than that of **2**. Compound **2** exhibits emission at 292 nm under the excited ultraviolet light of 271 nm (Fig. 8). Compound **2** and the free H_2CEPPA ligand exhibit very similar fluorescent emission bands which are attributed to an intraligand transition and are similar to those of other reported M—(H)CEPPA complexes [18, 19].

CONCLUSIONS

In summary, we present two double-layered metal carboxylate-phosphinate complexes $[Bi_2(\mu_3\text{-}O)(CEPPA)_2]_n$ (**1**) and $[Cd(HCEPPA)_2]_n$ (**2**). Compound **1** forms a *sql* (or Shubnikov tetragonal plane net) double layer based on the connection of $[Bi_4(\mu_3\text{-}O)_2(POO)_4(COO)_4]$ SBUs with —CH_2CH_2— spacers; while compound **2** is a (3,6)-connected *kgd* (or Shubnikov (3.6.3.6) double layer. The two distinct structures are mainly caused by differences in the metal centers and coordination modes of the (H)CEPPA ligands. Compounds **1** and **2** show high thermal stabilities, and their initial decomposition temperatures are at 373 and 303 °C respectively. The $[Bi_4O_2]$ unit causes fluorescence quenching in **1**, and compound **2** shows emission at 292 nm, which is assigned to intraligand transitions.

REFERENCES

1. *Whitesides G.M., Ismagilov R.F.* // Science. – 1999. – **284**. – P. 89.
2. *Lehn J.M.* // Science. – 2002. – **295**. – P. 2400.
3. *Cahill C.L., De Lill D.T., Frisch M.* // CrystEngComm. – 2007. – **9**. – P. 15.
4. *Maspoch D., Ruiz-Molina D., Veciana J.* // Chem. Soc. Rev. – 2007. – **36**. – P. 770.
5. *Robin Y., Fromm K.M.* // Coord. Chem. Rev. – 2006. – **250**. – P. 2127.
6. *James S.L.* // Chem. Soc. Rev. – 2003. – **32**. – P. 276.
7. *Carlucci L., Ciani G., Proserpio D.M.* // Coord. Chem. Rev. – 2003. – **246**. – P. 247.
8. *Fujita M., Tominag A.M., Hori A., Therrien B.* // Acc. Chem. Res. – 2005. – **38**. – P. 371.
9. *Melanie P., Darren W.J.* // Chem. Soc. Rev. – 2007. – **36**. – P. 1441.
10. *Ouellette W., Hudson B.S., Zubieta J.* // Inorg. Chem. – 2007. – **26**. – P. 4887.
11. *Mitzi D.B.* // Dalton Trans. – 2001. – **1**.
12. *Levchik S.V., Weil E.D.* // Polym. Int. – 2005. – **54**. – P. 11.
13. *Hu Q.S., Zhang X.Z., Luo S.F. et al.* // Acta Crystallogr., Sect. C. – 2011. – **67**. – P. o195.
14. *Xue J., Zhao C.C., Du Z.Y.* // Acta Crystallogr., Sect. C. – 2012. – **68**. – P. o355.
15. *Zhao C., Zhou Z.G., Xu X. et al.* // Polyhedron. – 2013. – **51**. – P. 18.
16. *Zhao C., Zhang J.W., Zhou Z.G. et al.* // J. Mol. Struct. – 2013. – **1033**. – P. 253.
17. *Dong L.J., Zhao C.C., Xu X. et al.* // Cryst. Growth Des. – 2012. – **12**. – P. 2052.
18. *Sun Y.H., Xu X., Du Z.Y. et al.* // Dalton Trans. – 2011. – **40**. – P. 9295.
19. *Zhao Y.P., Zhang J.W., Zhao C.C. et al.* // Inorg. Chim. Acta. – 2014. – **414**. – P. 121.
20. *Jawed A.* U.S. Patent 5750603, 1998.
21. *Kottke T., Stalke D.* // J. Appl. Crystallogr. – 1993. – **26**. – P. 615.
22. *APEX2*, Data Collection Software Version 2.1-RC13. – Delft, Netherlands: Bruker AXS, 2006.
23. *Cryopad*, Remote monitoring and control, Version 1.451. – Oxford, UK: Oxford Cryosystems.
24. *SAINT+*, Data Integration Engine v. 7.23a. © 1997—2005. – Madison, Wisconsin, USA: Bruker AXS, 2006.
25. *Sheldrick G.M.* SADABS v.2.01, Bruker/Siemens Area Detector Absorption Correction Program. – Madison, Wisconsin, USA: Bruker AXS, 1998.

26. *SHELXTLTM* Version 5 Reference Manual. – Madison, Wisconsin, USA: Siemens Engergy & Automation Inc., 1994.

27. *Wells F*. Three-Dimensional Nets and Polyhedra. – New York: Wiley-Interscience, 1977.

28. *Blatov V.A*. IUCr CompComm Newsl. – 2006. – **7**. – P. 4.

29. *Addison A.W., Rao T.N., Reedjik J. et al.* // J. Chem. Soc., Dalton Trans. – 1984. – P. 1349.

30. *Flack H.D.* // Acta Crystallogr. A. – 1983. – **39**. – P. 876.

31. *Briand G.G., Burford N., Cameron T.S.* // Chem. Commun. – 2000. – P. 13.

32. *Sadler P.J., Li H., Sun H*. // Coord. Chem. Rev. – 1999. – **185-186**. – P. 689.

33. *Thurston J.H., Swenson D.C., Messerle L.* // Chem. Commun. – 2005. – P. 4228.

34. *Gattow G., Schott D.* // Z. Anorg. Allg. Chem. – 1963. – **324**. – P. 31.

35. *Henry N., Evain M., Deniard P. et al.* // J. Solid State Chem. – 2003. – **176**. – P. 127.

36. *Sharutin V.V., Egorova I.V., Sharutina O.K. et al.* // Russ. J. Coord. Chem. – 2005. – **31**. – P. 2.

37. *Andrews P.C., Deacon G.B., Forsyth C.M. et al.* // Angew. Chem. Int. Ed. – 2006. – **45**. – P. 5638.

38. *Turova N.Y.* // Russ. Chem. Rev. – 2004. – **73**. – P. 1041.

39. *Chandler C.D., Roger C., Hampden-Smith M.J.* // Chem. Rev. – 1993. – **93**. – P. 1205.

40. *Nakamoto K*. Infrared Spectra of Inorganic and Coordination Compounds. – New York: Wiley, 1986.

41. *Deacon G.B., Philips R.* // J. Coord. Chem. Rev. – 1980. – **33**. – P. 227.

42. *Djordjevic C., Lee M., Sinn E.* // Inorg. Chem. – 1989. – **28**. – P. 719.

43. *Yua X.H., Zhang H.H., Cao Y.N. et al.* // J. Solid State Chem. – 2006. – **179**. – P. 247.

44. *Smet P.F., Van Gheluwe J., Poelman D. et al.* // J. Lumin. – 2003. – **104**. – P. 145.

45. *Folkerts H.F., Zuidema J., Blasse G.* // Chem. Phys. Lett. – 1996. – **249**. – P. 59.